Materials Advances

ROYAL SOCIETY OF CHEMISTRY

REVIEW

View Article Online
View Journal | View Issue

Cite this: *Mater. Adv.*, 2024, 5, 1772

Advances in the fabrication of potential nanomaterials for diagnosis and effective treatment of tuberculosis

Rehan M. El-Shabasy, *[ab] Moustafa Zahran, [bc] Ahmed H. Ibrahim, [d] Yasmin R. Maghraby[a] and Mohamed Nayel [e]

Tuberculosis (TB) is one of the fatal diseases amongst many other infectious diseases and is primarily caused by *Mycobacterium tuberculosis*. TB cases has been upsurging predominantly owing to the multi-drug resistance, which is also predicted to increase drastically in the near future. Hence, elaborate research exploring novel approaches for effective treatments has become an urgent area of study. In this regard, NP utilization has gained high recognition for the treatment and the effective/elaborate diagnosis of this fatal ailment. This review introduces a recent insight into novel NPs that have verified significant efficacy in TB treatment. Specifically, major focus has been placed on nanomaterials as optical probes for the diagnosis of TB. Gold, silver, and nickel oxide NPs as well as CdTe quantum dots have been investigated for the optical detection, and information about their studies is compiled herein. The sensing process is highly dependent on surface plasmon resonance, surface-enhanced Raman scattering, and/or on fluorescence emission. Overall, nanomaterials are considered a promising tool for developing sensors for the diagnosis of TB. Moreover, nanomaterials have gained significance for application in drug delivery approaches for treating TB, particularly mesoporous silica, which has shown to exhibit remarkable positive impacts on drug-resistant *M. tuberculosis*, delivering rapid and accurate diagnosis. However, most reported studies are missing intensive *in vivo* analysis. Limitations and future perspectives have been compiled and reported in this review article.

Received 16th September 2023,
Accepted 4th January 2024

DOI: 10.1039/d3ma00720k

rsc.li/materials-advances

1. Introduction

Currently, tuberculosis (TB) is one of the most globally widespread severe infectious diseases that leads to increased morbidity and mortality rates annually.[1] TB is the most common cause of death arising from a single bacterial entity, where 1.8 million patients have died from TB so far according to the World Health Organization data.[2] Globally, it is estimated that 10 million people have developed TB infection, and there are an estimated 1.8 million deaths annually due to primary disease, reinfection, or reactivation of the latent infection.[3] *M. tuberculosis* has a strong ability to adapt and survive in several host environments. It has a potential tendency to change its metabolic pathways and easily evade the host immune system through intracellular growth.[4] TB negatively affects the lungs (*i.e.*, pulmonary TB) and the central nervous system (CNS), causing severe meningitis.[5]

TB is primarily caused by *Mycobacterium tuberculosis*, which is a type of bacteria that can be identified as either Gram-positive or Gram-negative on a gram stain.[6] Several clinical approaches have reported the diagnosis of TB, encompassing culture of the tracheal aspirate, cerebrospinal fluid (CSF), gastric washings, chest X-ray, and skin examination.[7]

Diverse antibiotics could be used along with other medications for treating TB.[8] Several medications such as rifampicin, isoniazid, ethambutol, kanamycin, capreomycin, amikacin and pyrazinamide were approved by the FDA for the treatment of infections caused by *M. tuberculosis*,[9] as shown in Table 1. Utilizing a fixed dosage can possess several advantages, including cost-effectiveness, reduction in the pill burden and logistical benefits.[10] However, it also has several disadvantages such as poor bioavailability, enzyme level elevation, adverse drug reactions, questionable effectiveness in the absence of directly observed therapy short (DOTS) course and therapeutic drug

[a] *Chemistry Department, The American University in Cairo, AUC Avenue, New Cairo 11835, Egypt. E-mail: rehan.elshabasy@aucegypt.edu*
[b] *Department of Chemistry, Faculty of Science, Menoufia University, Shebin El-Kom 32512, Egypt*
[c] *Menoufia Company for Water and Wastewater, Holding Company for Water and Wastewater, Menoufia 32514, Egypt*
[d] *Center for Materials Science, Zewail City of Science and Technology, 6th of October 12578 Giza, Egypt*
[e] *Department of Animal Medicine and Infectious Diseases, Faculty of Veterinary Medicine, University of Sadat City, Egypt*

Table 1 The most commonly used antibiotics for TB treatment along with their dosage limits

Type of TB	Drug	Dosage (mg kg^{-1} day^{-1})	Max. dosage (mg)	Ref.
1st line	Rifampicin	10 (adults) 10–20 (children)	600 300	16–18
	Isoniazid	5 (adults) 10–20 (children)	 2000	
	Pyrazinamide	1000 (40–55 kg) 1500 (56–75 kg) 2000 (≥76 kg) 15–30 (children)	N/A	
	Ethambutol	800 (40–55 kg) 1200 (56–75 kg) 1600 (≥76 kg) 15–20 (children)	1600 1000	
	Moxifloxacin	400 (≥12 years of age)	N/A	
2nd Line	Levofloxacin	15–20 (<15 years) 250–750 mg tab (for a weight <30)	1.5 g	16 and 19
	Amikacin	10–20 (<15 years) 500 mg/2 mL vial	1 g	
	Clofazimine	2–5 (<15 years) 50–100 (>15 years)	100	
	Capreomycin	15–20 (<15 year) 500 (>15 years)	1 g	
	Gatifloxacin	400 (for adults only >18 years) 10–15	1 g	
	Moxifloxacin	400 15 (<16 kg)	400 800	
	Streptomycin	15–20 (<30 Kg) 400 (<30 Kg)	1 g	
	Gatifloxacin	Not used in <18-year olds	800	

N/A: not applicable.

monitoring, as well as difficulty in dose adjustments. Accordingly, there is an urgent need to reassess the current treatment regimen; otherwise, conversion of TB into multi-drug resistant TB or extensively drug resistant TB might occur. Selecting an effective treatment plan and drug dosage depends on several factors, including whether the patient has an active or latent disease, type of TB, general health of a patient, and finally the patients' age range (Table 1).[10]

TB is very challenging to be efficiently treated, demanding lengthy chemotherapy sessions and multi-drug regimens.[11] The needed duration for an effective treatment is very long, varying from six months for drug-susceptible infection to more than two years for multi-drug resistant TB.[12] Almost 30% of the world's population is infected by harsh infections.[13] The risk of TB has dramatically increased lately, which has triggered researchers to develop new ways of rapid detection and efficient treatment regimens. While treating TB, drug resistance is the main obstacle causing several severe health risks.[14,15] Recently, the availability of new drugs namely, bedaquiline, delamanid and repurposed drug linezolid, clofazimine and carbapenems, are being used more frequently in drug-resistant TB regimens.[9]

The impacts of drug-resistant and multidrug-resistant cases are particularly associated with the most challenging threats towards TB control owing to the minute cure rate. Therefore, most current reports suggest exploring more effective therapies and developing research motivation towards the search for surrogate treatment approaches.[20] The hepatotoxic effects of many drugs, such as rifampicin, isoniazid, pyrazinamide, and ethambutol, which are all first-line anti-tubercular medications, should be considered. Elevations in liver functions were observed in several cases. Stopping the medication can reverse aminoglycoside-induced nephrotoxicity.[21] The occurrence of renal toxicity depends on the presence of any underlying renal disease in the patient and the dosage of the medication being administered.[22] In addition, most second-line antituberculosis drugs (*e.g.* ethionamide, capreomycin, linezolid, amikacin, levofloxacin, gatifloxacin, kanamycin, streptomycin, cycloserine, and moxifloxacin) that are possessing poor efficacy are generally toxic and require prolonged treatment durations; compromising the patient's adherence and therapeutic drug monitoring.[19] Antituberculosis combinations refer to the administration of multiple drugs concurrently to treat tuberculosis. These drugs have distinct mechanisms of action, which help prevent the development of drug-resistant strains of *M. tuberculosis*.[23] By targeting the bacteria in various ways, the use of medications with different mechanisms of action enhances the effectiveness of treatment by helping to shorten the duration of treatment, decreasing the chances of disease release, and minimizing the development of drug resistance, which is not normally achievable with monotherapy.[24]

Considering the merits of the high capacity for engineering functional systems at the molecular scale, nanotechnology has gained much significance for application in several materials on a molecular, atomic, and supramolecular scale, including industrial and medical applications.[25] Nanomaterial-based nanomedicines are widely involved in various clinical aspects

owing to their bioavailability, enhanced activity, dose-responsiveness, targeted ability, personalization, and high safety when compared to conventional medications.[26,27] NPs have been extensively utilized as nanomedicines for disease-efficient treatment and exploited as novel alternatives for nano-based medicines for TB successive diagnosis.[20] The intelligent usage of NPs alongside antimicrobial substances has received significant research attention in this context. NPs possess a high surface area, entailing several active sites, which increase their affinity to interact with a broader spectrum of biological entities.[28] NPs have also been reported to exhibit high penetrability among various tissues.[29] Recently, several NPs have emerged to be applied positively as anti-TB agents, including Ag NPs, Au NPs, and ZnO NPs.[30–32] Furthermore, NPs could be utilized as electrochemical and optical probes for the diagnosis of tuberculosis.[33,34] The electrochemical-based sensors depend on the electrochemical behaviour of NPs at the electrode surface, while the optical-based sensors are mainly based on the surface plasmon resonance (SPR), excitation emission, and surface enhanced Raman scattering (SERS) of NPs, such as gold, silver, nickel oxide, and cadmium telluride.

The current review outlines the role of fabricated nanomaterials and NPs in the optical diagnosis and treatment of tuberculosis in comparison to traditional methods. Additionally, this review compiles information about different nanomaterials, mainly silica mesoporous, in overcoming multiple barriers associated with the delivery of medications during tuberculosis therapy.

2. Potential nanomaterials for effective treatment

Currently, several well-established anti-TB agents (*e.g.*, isoniazid, rifampicin, pyrazinamide, ethambutol, *etc.*) are broadly used; however, several problems are associated with using these drugs, such as toxicity and poor efficacy during treatment.[35] Consequently, there is an urgent need for novel effective and safe alternatives. Nanomaterials have attracted significant attention as potential candidates for overcoming the obstacles of typically applied commercial antibacterial agents, particularly their high resistance and therapeutic limitations. In this context, several academic experts have released many investigations worldwide involving natural biopolymers that have been successfully manipulated in the fabrication of anti-TB drugs. This type of drug has gained high interest recently because of its remarkable properties, including biocompatibility, biodegradability, and non-toxicity.[35] For instance, the facile, scalable, and cost-effective method has recently been applied in the fabrication of chitosan biguanidine NPs as an anti-TB drug.[35] Predominantly, the synthetic approach was distinguished in which uniformly well-distributed particles were significantly formed with a small particle size (38 nm). The examination test showed potential inhibition growth against sensitive, MDR, and XDR *M. tuberculosis* pathogens (MIC: 0.48, 3.9, and 7.81 μg mL^{-1}) compared to chitosan NPs (15.63, 62.5 > 125 μg mL^{-1}) and the commercial isoniazid drug (0.24, 0, and 0 μg mL^{-1}),

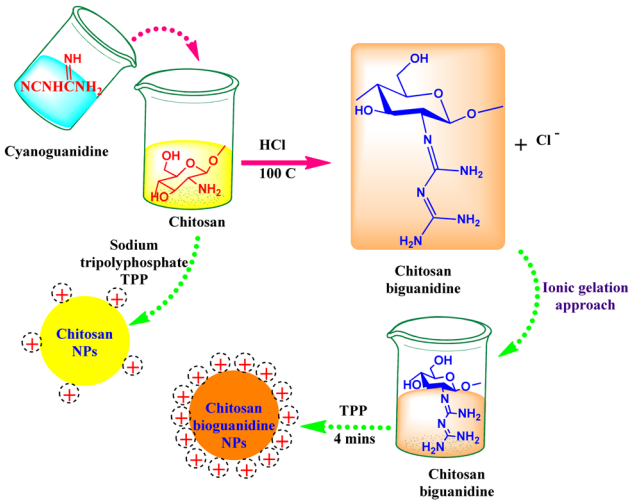

Fig. 1 Ionic gelation method for the synthesis of chitosan biguanidine NPs and unmodified chitosan in the presence of TPP. The cloud of positively charged guanidine surrounded by chitosan through condensation significantly enhances the antibacterial efficacy.

respectively.[35] This remarkable effect could be attributed to the high density of positively charged grafted biguanidyl groups located on the surface of chitosan chains, which demolished the bacterial cell wall by strong electrostatic interactions, as shown in Fig. 1. In addition, it is worth mentioning that the polycationic guanidine polymers possess an efficient antibacterial efficacy because of the highly positive charges of amine groups, which are strongly attached to the negative charges on the bacterial cell membrane, resulting in bacterial death without leading to microbial resistance. It also revealed high selectivity towards bacterial cell membranes owing to the electrical neutrality of the outer membrane of mammalian cells.[36,37]

Several reports have shed light on the phyto-fabrication of NPs from natural sources, particularly from planta.[20,38] ZnO NPs have attracted attention as a potential novel practical method for TB treatment (Table 2).[20] In that context, phyto-fabricated ZnO NPs from the aqueous extract of *Canthium dicoccum* have been reported with an average size of 33 nm. The inhibition efficiency of the biosynthesized ZnO NPs was induced at 25 μg mL^{-1} owing to its high specific surface charge and the generation of reactive oxygen species (ROS).[39] It is noteworthy that only few reports have examined the action mechanism concerning ZnO-NPs against *M. tuberculosis.* The interaction between ZnO-NPs and sulfur or phosphorous bases has been reported to efficiently deprive the DNA ability of replication.[40] Patil *et al.* also reported the exact action mechanism as Taranath, who investigated the green synthesis of ZnO NPs using *Limonia acidissima* L. with a controllable size between 12 nm and 53 nm.[38] The prepared ZnO NPs were directly attached to the bacterial surface and then easily penetrated the cell membrane. The small particle size assists the particles in entering into the cytoplasm of mycobacterium *via* endocytosis and deactivates the essential enzymes required for adenosine triphosphate production[41,42] (Fig. 2). Accordingly, ROS are generated; eventually, bacterial cell apoptosis is

Table 2 List of recent novel applied nanomaterials used as anti-TB drugs

Nanomaterials	Fabrication method	Particle size (nm)	Results	Ref.
Chitosan biguanidine NPs	One-pot/ionic gelation	38	MIC: 0.48, 3.9, 7.81 μg mL^{-1} for sensitive, MDR, and XDR *M. tuberculosis*	35
ZnO NPs		33	TB inhibited at 25 μg mL^{-1}	39
ZnO–Se NPs	Hybridization of zinc oxide and selenium	90	Suppressed ATP production Increased ROS production Distortion of the membrane structure	3
Se-NPs		70–100	Destroy the integrity of the cell envelope	46
ZnO NPs	Phytosynthesis	12–35	Control the growth of *M. tuberculosis* at 12.5 μg mL^{-1}	38
Alginate modified-PLGA NPs	—	312–365	2s line anti-TB drugs were incorporated into alginate modified PLGA NPs. Improved entrapment and controlled release of the drugs by modifying PLGA with alginate reflected in the synergistic effect of the dual entrapment of moxifloxacin and amikacin compared to single-drug-loaded NPs	51
Graphene-TMC-CMS IPN NPs	One-pot ultrasonication	22	MIC values of 0.98, 3.9, and 7.81 μg mL^{-1} for inhibiting the growth of sensitive, MDR, and XDR *M. tuberculosis* pathogens compared to the bare TCNPs (7.81, 31.25, >125 μg mL) and the isoniazid drug (0.24, 0, 0 μg mL^{-1}), respectively	52
TMC-Ag	One-pot green synthesis	11–17.5	Antitubercular activity of nanocomposite was evaluated against both *M. tuberculosis* and lung carcinoma cells (A-549). MIC inhibited *M. tuberculosis* of 1.95 μg mL^{-1}.	53

initiated.[43] ZnO NPs can interact with sulfur or phosphorus-containing soft bases, including RS–, R–S–R, R–SH, and PR3, which inhibit the replication of DNA.[40,44] Therefore, the sulfur-containing protein in the membrane or inside the cell and phosphorus-containing elements, such as DNA, are proposed to be favorable positions for the effective action of ZnO NPs.[40] An additional suggested mechanism referred to as lipid metabolism interference causes cell destruction and apoptosis.[45]

Although there are only few reported data discussing the practical action mechanism of ZnO NPs, they have massive effects on TB treatment. Consequently, further intensive research could reveal a new era of the actual mechanism through diverse elaborate *in vivo* studies. Moreover, the potential efficiency of selenium NPs (SeNPs) has been examined, in which the formed NPs have verified a distinguished recognition against the inhibition of *M. tuberculosis* growth by demolishing the integrity of the cell envelope.[46] The anti-microbial effect of SeNPs against *M. tuberculosis* was estimated to have a lower toxicity effect.[47] The feasible mechanism of bactericidal activity could result in the arrest of the cell cycle, instigating a notable degree of apoptosis.[48] Se NPs were also chosen as potential therapeutic materials with lesser side effects.[49]

Intensive efforts are still in progress by researchers to explore more efficient anti-TB-drug-based NP materials. In this

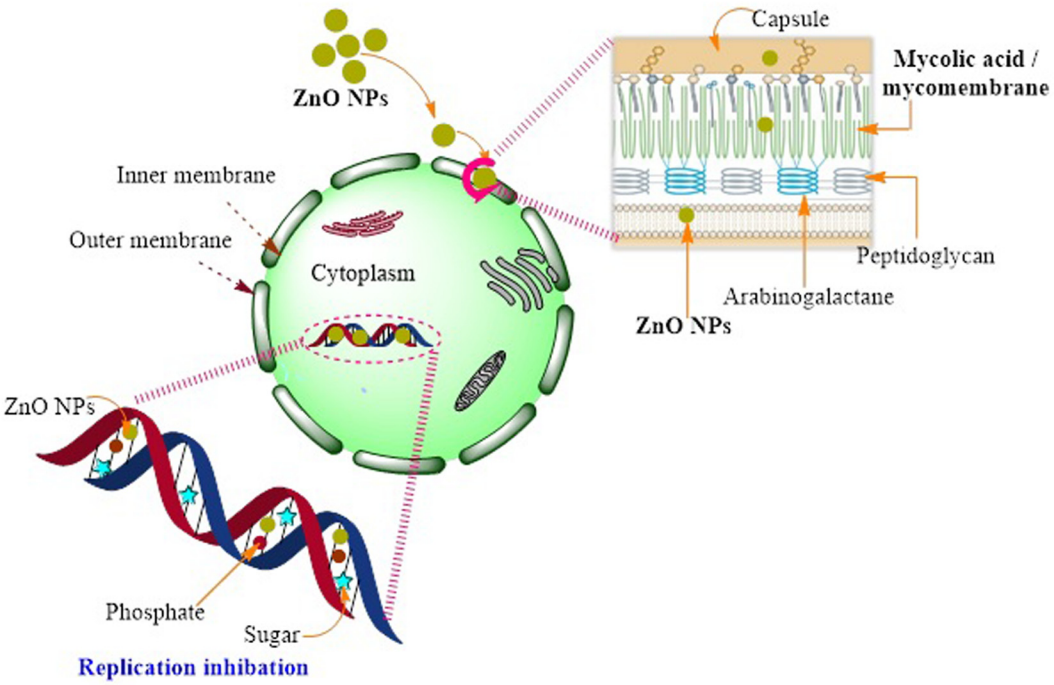

Fig. 2 Schematic diagram representing the possible action mechanism of ZnO NPs resulting in the loss of DNA replication in *M. tuberculosis*.

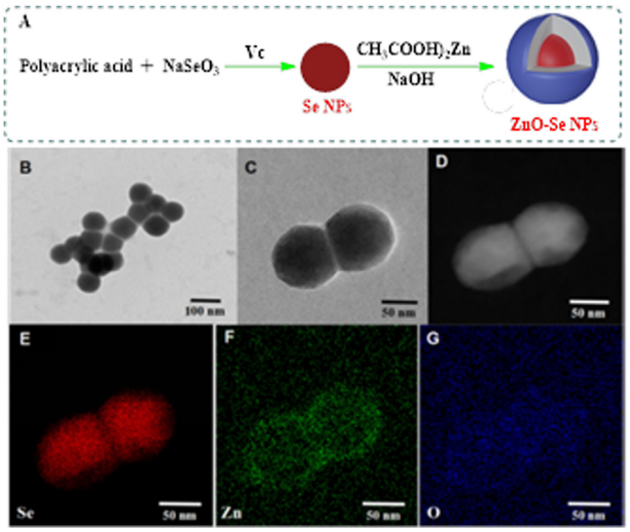

Fig. 3 Preparation and characterization of ZnO–Se NPs. (A) Schemes for the preparation of ZnO–Se NPs. (B) and (C) Typical TEM images of ZnO–Se NPs. (D) Typical TEM-EDS dark field image of ZnO–Se NPs. (E) Typical TEM-EDS selenium (Se) mapping analysis of ZnO–Se. (E) Typical TEM-EDS selenium (Se) mapping analysis of ZnO–Se NPs. (F) Typical TEM-EDS zinc (Zn) mapping analysis of ZnO–Se NPs. (G) Typical TEM-EDS oxygen (O) mapping analysis of ZnO–Se NPs. With permission from ref. 3.

regard, a remarkable development has recently been reported considering the discriminant features of both ZnO and Se NPs.[3] A novel hybridization approach was involved in fabricating spherical ZnO–Se core–shell NPs, as presented in Fig. 3.[3] Undoubtedly, the designed NPs depend on utilizing and combining the antibacterial advantages of both Se and ZnO by engineering novel potential alloy NPs. The average diameters of the fabricated ZnO–Se NPs were measured to be 90 nm, which stimulated potential killing effects against extracellular *M. tuberculosis*, including BCG and virulent H37Rv. The obtained core–shell NPs can strongly suppress ATP production, enhancing the creation of intracellular ROS and accordingly distorting the membrane's structure. Interestingly, intracellular inhibition growth could also be exhibited by promoting M1 polarization to enhance antiseptic nitric oxide production and developing apoptosis and autophagy of *M. tuberculosis*-infected macrophages by increasing the intracellular ROS, disrupting mitochondria membrane potential and inhibiting PI3K/Akt/mTOR signaling pathway.[3]

A novel host-directed therapy for multidrug-resistant tuberculosis was examined.[50] Moxifloxacin and amikacin were incorporated into PLGA NPs *via* an encapsulation process. Two nanocomposites, alginate-entrapped PLGA NPs and alginate-coated PLGA NPs were produced using a water-oil–water emulsion method, as depicted in Fig. 4. The results showed the potential encapsulation performance of two hydrophilic second-line anti-TB drugs, and intra-macrophage delivery of the synthesized nanosystem utilized significantly for rapid treatment of multi-drug resistant. The coated NPs showed undesirable particle sizes measured at a particle size of 640 ± 32 nm.

The large size distribution was possibly caused by the high viscosity of the external alginate phase, which formed larger emulsion droplets, eventually leading to greater particle size ranges.[51] In contrast, PLGA NPs entrapped within alginate-induced spherical favorable particle sizes ranged from 312 to 365 nm, which enhanced their use for internalization into alveolar macrophages (Fig. 4). The loading efficiency of moxifloxacin was found in the range of 10.1–18.7 μg mg^{-1}, whereas amikacin was in the range of 15–17.4 μg mg^{-1} compared to non-modified PLGA NPs, that revealed a significantly less amikacin loading of 6.2 μg mg^{-1} polymer and 4.2 μg mg^{-1} of moxifloxacin. The entrapped nanocomposite presented potential inhibition activity against *M. tuberculosis*-infected macrophages compared with the single-loaded drug NPs or untreated cells.[51]

In addition, a new category of distinguished nanomaterials has emerged in multi-functional applications, principally the inhibition of tuberculosis infection. For instance, a highly biocompatible graphene layer was engineered and decorated with *N*,*N*,*N*-trimethyl chitosan (TMC)/carboxymethyl starch (CMS) interpenetrating polymer networks (IPN) *via* a green and a one ultrasonic pot strategy.[52] TEM analysis revealed a uniform distribution of TMC-CMS hydrogel NPs on graphene surfaces with a small particle size of 22 nm, which was roughly compared to the pure NPs formed at 30 nm. The inhibition activity of the synthetic nanocomposite was evaluated against different *M. tuberculosis* pathogens with MIC values of 0.98, 3.9, and 7.81 μg mL^{-1} for sensitive, MDR, and XDR compared to the bare TCNPs (7.81, 31.25, and >125 μg mL^{-1}) and the isoniazid drug (0.24, 0, and 0 μg mL^{-1}), respectively. This reveals a considerable synergism in the antituberculosis activity between TCNPs and graphene nanosheets.[52] In that context, the same biodegradable polymer (TMC) as Ag NPs has been examined for the first time against tuberculosis disease, where some limitations arose that are associated with Ag NPs, including high toxicity and poor stability.[53] In contrast, TC NPs with graphene nanosystems have been exploited to be applied safely as an excellent anti-TB drug.[52]

From previous literature and some relevant studies, all the reported data confirmed the promising effects of NPs, which efficiently enhanced further *in vivo* studies. It is noteworthy that the data tabulated revealed a significant efficiency of most fabricated NPs, particularly those small particles whose size ranged from 20 to 100 nm.

3. Nanomaterial-based optical sensors for tuberculosis detection

Currently, nanomaterials are being incorporated into chemical sensors to elevate their sensitivity, improve their selectivity, and lower their detection limits. For example, nanomaterials have been extensively used for constructing electrochemical sensors for detecting pesticides,[54,55] dyes,[56,57] and biological molecules[58] as well as optical sensors to detect analytes, such as glucose,[59] polyphenols,[60] pesticides,[61] metal ions,[62] crude oil,[63] and microorganisms.[64,65]

Nanomaterials have been widely utilized in the fields of biomedicine and bioengineering. For instance, they have been

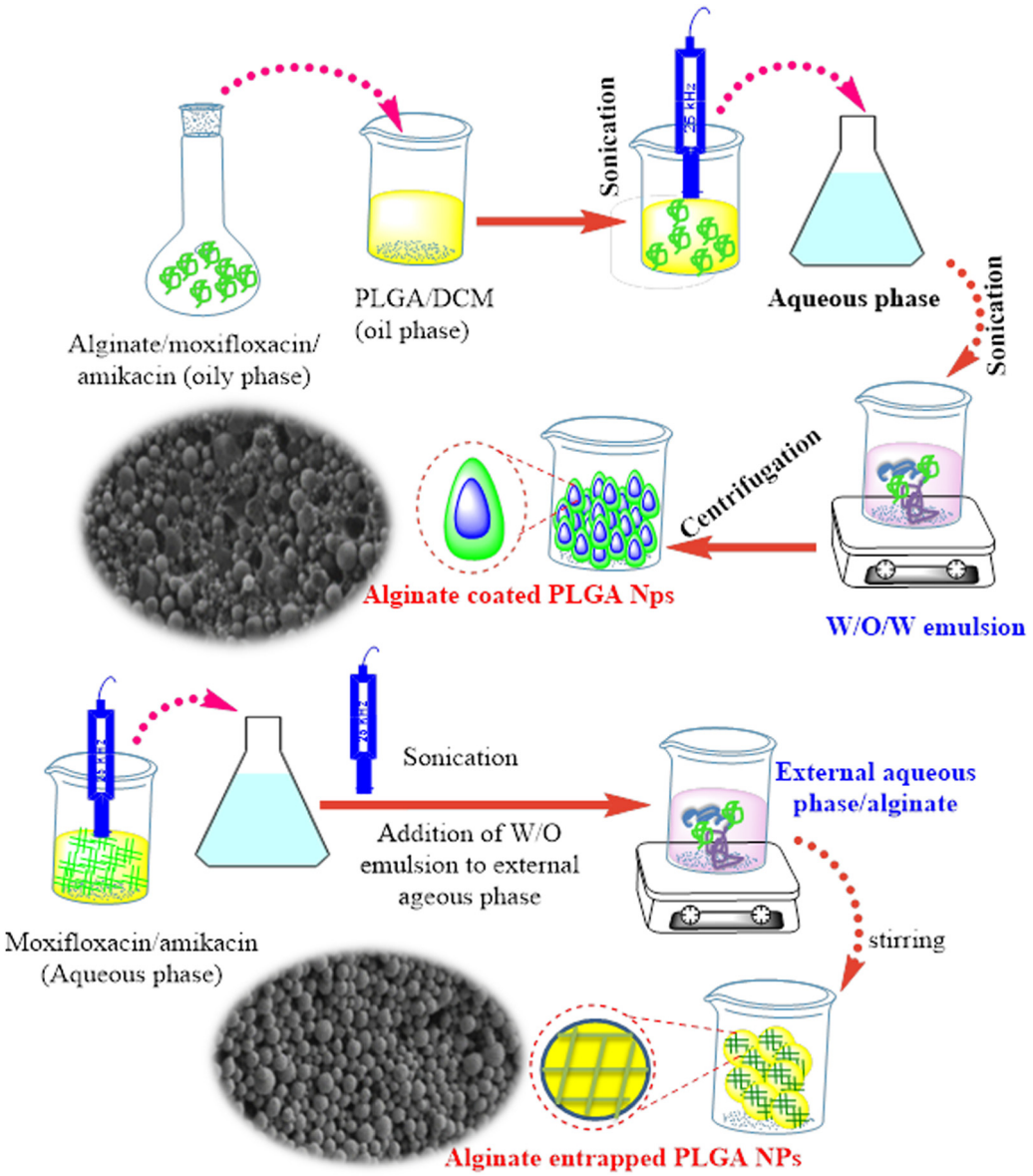

Fig. 4 Schematic presentation of alginate entrapped PLGA nanoparticles and alginate-coated PLGA NPs along with their respective SEM images.[51]

used in the field of the medical diagnosis of several diseases, including tuberculosis.[66] They were incorporated into electrochemical and optical sensors for elevated sensitivity and better selectivity towards tuberculosis.[67,68] Fig. 5 lists the nanomaterials used in the optical detection of tuberculosis. In this review, a great focus has been placed on nanomaterials, such as Au nanoparticles (NPs), Ag NPs, cadmium telluride quantum dots (CdTe QDs), and nickel oxide (NiO) NPs, that are particularly used for the optical detection of tuberculosis. The sensing strategy is based on attractive physical phenomena, such as SPR-, SERS, and fluorescence emission. Table 3 lists the nanomaterial-based optical sensors used in the optical detection of tuberculosis.

3.1. Au NPs

Au NPs, which normally possess distinctive optical properties, are incorporated into optical sensors.[69,70] Au NP-based optical

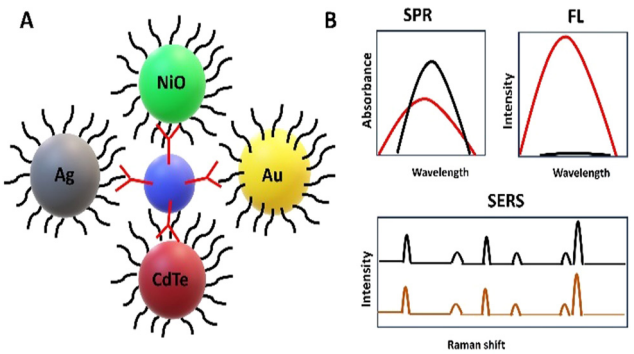

Fig. 5 Schematic representation of the nanoparticles used in the optical detection of tuberculosis (A) and the corresponding optical signals (B).

Table 3 Nanomaterial-based optical sensors for tuberculosis diagnosis

Nanomaterial	Type of optical sensor	Mechanism	Detection limit	Ref.
AuNPs	SPR	Biosensing (antigen)	ND	73
Au layer	SPR	ND	ND	74
Ag NPs	SERS	ND	ND	79
	SERS	ND	ND	80
Ag NPs/$BaTiO_3$	SPR	ND	ND	81
CdTe QDs	Fluorescence	Biosensing	35 pM	86
	Fluorescence	Biosensing	0.3 ag mL^{-1}	85
NiO NPs	SPR	Biosensing (antibody)	0.1 ng mL^{-1}	88

SERS: surface-enhanced Raman spectroscopy, SPR: surface plasmon resonance, QDs: quantum dots, and ND: not defined.

sensors have been used for targeting many biological molecules[59,71] and water pollutants.[72] These can also be used for the diagnosis of tuberculosis. Recently, Au NPs, which were conjugated with goat anti-rabbit IgG H&L secondary antibody for improving the detection signal, have been incorporated into optical biosensors for detecting tuberculosis antigens. Additionally, mycolic acid was adsorbed onto the surface of the sensor to capture the tuberculosis antibodies. In the presence of anti-*mycobacterium tuberculosis* antibodies, the refractive index change resulted in reduced transmitted intensity, making the SPR platform appropriate for the diagnosis of tuberculosis.[73] Additionally, an SPR-based nano sensor has been developed for detecting tuberculosis using an Au layer of 50 nm thickness as a plasmonic substance. MoS_2 was adsorbed on the Au layer to strengthen the coupling between the core mode and the surface plasmon polariton mode of the fiber, while MXene was used as a biorecognition element.[74]

3.2. Ag NPs

Ag NPs are being employed in various environmental and medical applications.[75,76] For example, they were used for electrochemical and optical detection of numerous analytes.[77] Their ability to detect target analytes is attributed to their significant optical features.[78] Previously, Ag NP-based optical sensors were examined as effective tools for detecting tuberculosis. For example, the SERS sensor was constructed based on Ag NP interactions with *Mycobacterium tuberculosis* cells. The sensor depended on using bacterial cells as templates for the synthesis of Ag NPs. The electrostatic interactions between Ag^+ ions and the bacterial cells lead to strong and reproducible SERS spectra.[79] Additionally, an Ag NP-based SERS sensor was used to identify tuberculosis. Ag NPs are capable of differentiating between bacteria, such as tuberculosis and typhoid, which have similar symptoms.[80] However, an SPR sensor, which is based on an Ag layer of 65 nm, a barium titanate ($BaTiO_3$) layer of 9 nm, and two graphene layers, is also applied for detecting tuberculosis. Increasing the thickness of the Ag layer improved the transfer of incident light energy to the surface plasmon, leading to efficient excitation of the surface plasmon.[81]

3.3. CdTe QDs

CdTe QDs are utilized in various applications, including catalysis,[82] solar cells,[83] and sensors.[34,84] Recently, they have been proven to be effective materials in optical biosensors for detecting tuberculosis.[85,86] QDs, which have brilliant luminous properties, were utilized for labelling single-stranded DNA (ssDNA), which is complementary to the IS6110 gene fragment of *M. tuberculosis*. The QD-DNA acts as a fluorescence donor, while Cu-TCPP, a two-dimensional metal organic framework, acts as an acceptor. In the absence of the tuberculosis gene, the fluorescence of QDs-DNA was quenched because of the affinity of Cu-TCPP towards ssDNA, while in the presence of the target gene, DNA hybridization occurred, and the fluorescence was maintained in a target-concentration-dependent manner.[86] However, CdTe QDs are used as aptameric sensors for detecting Interferon-γ, which is essential in the diagnosis of tuberculosis. The sensing strategy is based on the fluorescence properties of QDs.[85]

3.4. NiO NPs

NiO NPs are gaining great attention in different research fields owing to their distinctive desirable features and properties.[87] Previously, an SPR immunosensor based on NiO NPs was applied for the detection of tuberculosis. The sensing process depended on the amplification power of the NPs.[88]

4. Drug delivery for rapid diagnosis

Even with superior technological advancements in novel diagnostic techniques and the discovery of several antibiotics, TB remains a critical challenge that could produce threats to human health. The early diagnosis problem is worsened due to the non-rapid prognosis that is maintained until present in clinics, in addition to the unavailability of new antibiotics for decades. The ever increasing incidences displayed inefficient and rapid diagnostic procedures along with a lack of satisfactory treatments.[30] There is an unmet demand for designing new diagnostic and treatment approaches to overcome TB-related hazards, also to obtain a smooth treatment and to prevent TB as well. Ideally, novel methods should be developed to develop sensitive, cost-effective, rapid diagnosis, treatment, and prevention. Currently, clinicians can diagnose TB in various ways, including sputum smear microscopy, immunological methods, rapid molecular tests, culture-based techniques, the use of chest X-rays, CT scans, polymerase chain reaction (PCR), and real-time PCR, as presented in Fig. 6. Even though these methods are versatile approaches designed and developed by researchers for a rapid and accurate diagnosis, there is a need to design more rapid, highly sensitive, and cost-effective TB tests.[4,89]

Throughout this regard, NPs have shown significant results in the rapid diagnosis and treatment of TB. Similarly, mesoporous materials have gained interest in being applied as nanodrug delivery systems owing to their unique surface features and high biocompatibility.[90] Their highly ordered networks and porous surface structures make them an optimum choice for nanomedicine applications. Several reports have recently investigated the efficacy of silica mesoporous nanocarriers against

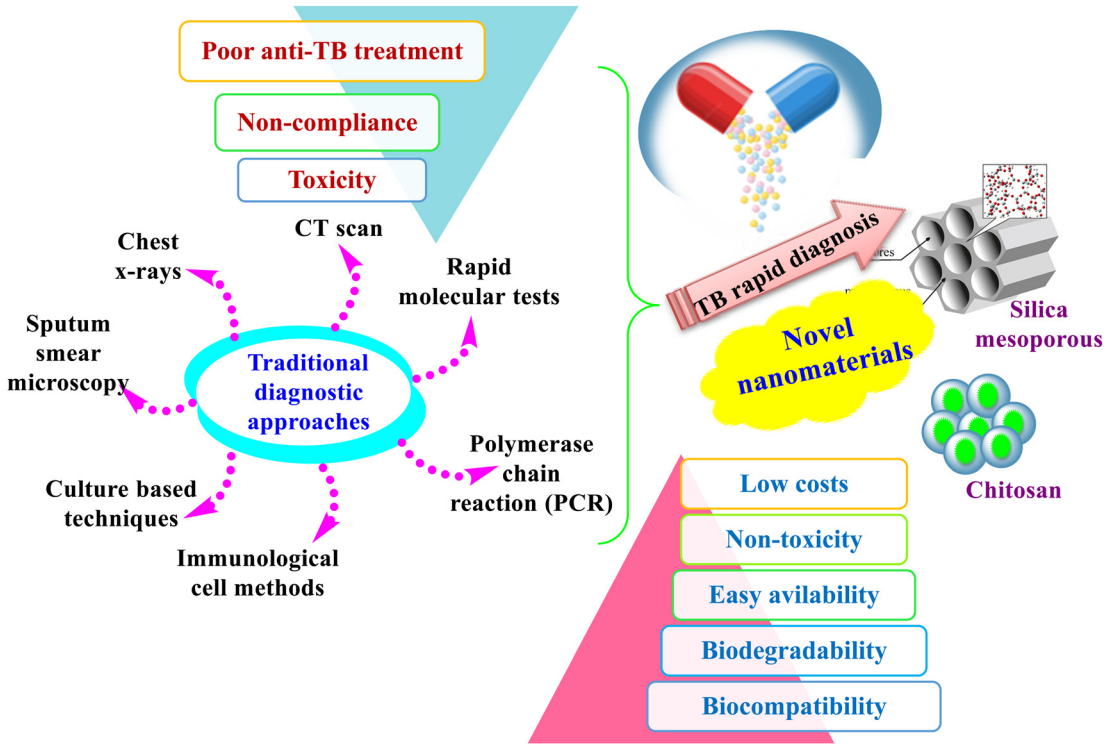

Fig. 6 Traditional approaches and novel nanomaterials applied for TB diagnosis.

TB. For instance, mesoporous silica NPs containing gold (MSNs@GNPs) were recently developed as novel nanocarriers aiming for a rapid diagnosis. The *in vitro* studies of the prepared material showed a superior effect against *M. tuberculosis*, particularly at a lower MIC. The fabricated composite showed a dual effect for the rapid diagnosis and treatment of TB, so it is highly recommended for use in clinical *in vivo* studies.[5] A similar study has recently confirmed the high tendency of silica mesoporous NPs towards high loading efficiency to be one of the best options for drug loading resistance purposes.

Ag NPs have proven to have great bactericidal activity. Nevertheless, several obstacles have limited their potential wide applications, particularly their relatively high toxicity, which urges nanocarrier engineers to enable the safe delivery of silver-based NPs to their targets in the cells. In this regard, mesoporous silica NPs are potentially utilized as carriers of AgNPs as antimycobacterial drugs against *M. tuberculosis*.[91] Two synthetic methods have been designed so far for the efficient fabrication of a 2D hexagonal mesoporous silica nanosystem and Ag–Si core–shell. AgBr NPs were incorporated into the holistic silica network. In contrast, the mesoporous silica was surrounded by metallic AgNPs as the inside core in a radial mesoporous rearrangement, as shown in the TEM images (Fig. 7). Both fabricated nanosystems exhibited antimycobacterial capacities in the *in vitro* study, induced by damaging the cell envelope, being lower than the MIC for the nanosystem including AgBr.[91]

Moreover, a more critical *in vivo* study was conducted by successfully loading the antimicrobial peptide NZX into silica mesoporous particles as an efficient carrier. The results revealed an elevated inhibition of the intracellular mycobacteria in primary macrophages and maintained the ability to destroy *M. tuberculosis in vivo* in a murine model.[4] In this context, NZX was previously introduced as a novel antimycobacterial agent, which induced promising efficacy in killing clinical and multi-drug resistant strains of *M. tuberculosis* at various ranges of therapeutic concentrations.[92] This peptide verified a substantial reduction in the bacterial load of infected mice lungs after five days when compared to Isoniazid and Rifampicin, which needed substantial durations of treatments (*i.e.*, six months to two years along with a multi-drug resistance). The reported data analysis confirmed the excellent efficiency potential of the applied mesoporous silica that upgraded NZX intracellular delivery and mycobacteria inhibition.[4,92] To the best of our knowledge, this study is the only one that has investigated the actual performance of nanocarriers under *in vivo* trials specifically. Most of the reported studies revealed the significant and efficient role of silica-based materials in the drug delivery of anti-TB drugs. However, other researchers have eagerly tried to determine additional ingredients to be applied as effective nanocarriers. For example, a polyethylene glycol and chitosan mixture were designed to encapsulate rifampicin using an ionic gelation technique as a drug delivery model. The features and surfaces of the produced NPs were changed *via* strong bindings between the chitosan and polyethylene glycol, in which the particle size was actually increased; and consequently, drug encapsulation was also enhanced.[93] This interaction also prolonged the capsulated rifampicin retention duration when compared to

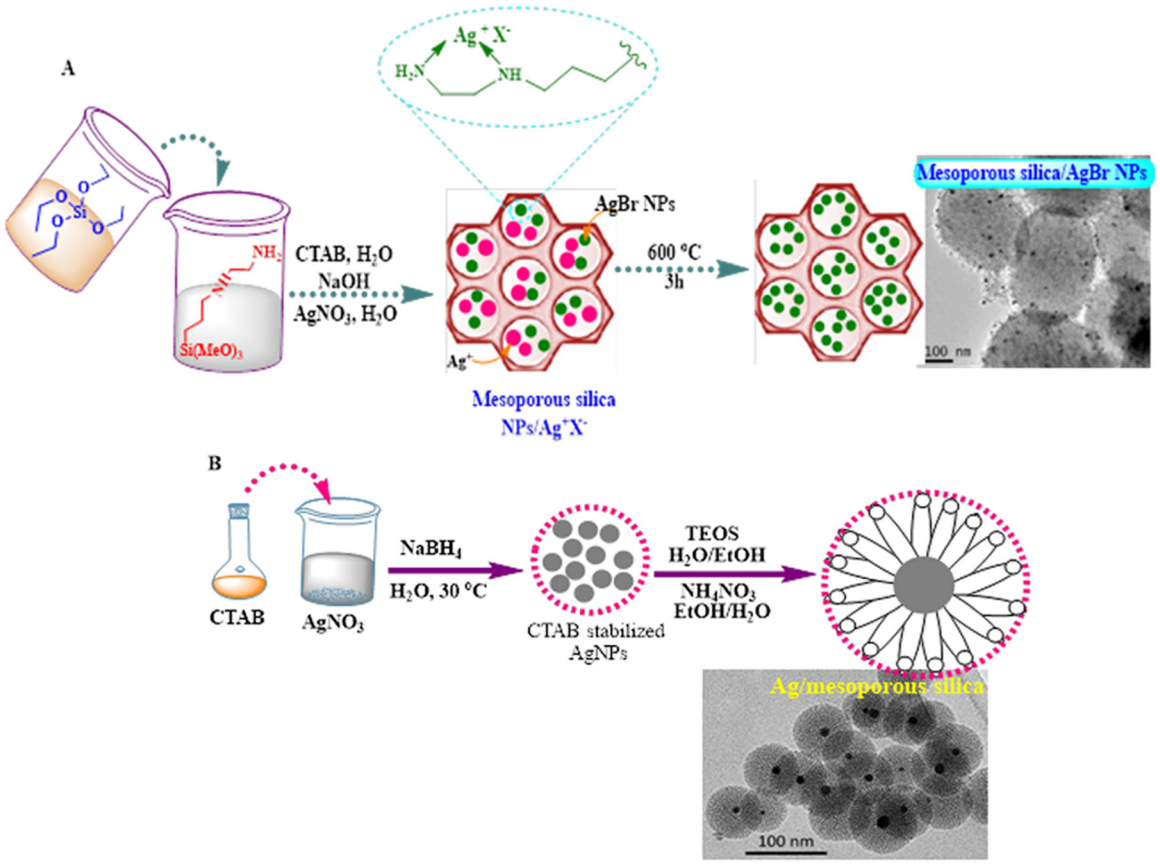

Fig. 7 Scheme of the synthesis of (A) mesoporous silica nanoparticles containing silver bromide nanoparticles (MSNs-AgBrNPs), following a one-pot incorporation method of silver ions and subsequent thermal treatment and (B) core@shell type nanoparticles consisting of silver coated with mesoporous silica (Ag@MSNs) and TEM images of the both formed nanosystems.[91]

the non-coated drug. The results also discussed *in vitro* drug release, which depended on the initial drug concentrations.[93] Biodegradable polymers are appreciated candidates and manipulated to be used as drug delivery nano carriers for sustainable drug release. A novel amphiphilic chitosan-grafted-(cetyl alcohol-maleic anhydride-pyrazinamide) was fabricated to entrap Ag NPs and rifampicin *via* dialysis.[94] The developed nanosystem promoted the encapsulation effectiveness of the low-soluble drug (rifampicin with AgNPs) by increasing the hydrophobicity of the inner core of the prepared micelle. The *in vitro* cell viability, cell apoptosis and cellular uptake examination displayed that a multi-drug delivery system improved the biocompatibility and increased the cytotoxicity on the cells.[94] Finally, all the discussed reports so far have proven the remarkable impact of nanomaterials as a promising system for the safe drug delivery of anti-TB agents.

5. Limitations and future perspectives

Several scientific reports and research works have stressed the ubiquitous green fabrication techniques of diverse nanomaterials from plants; however, manipulation of biowastes incorporated in synthesizing nanomaterials as anti-TB drugs is yet to be elaborately studied/reported. Biowaste recycling could open up a new era of research for innovative new drugs for the rapid diagnosis and treatment of TB through eco-friendly and cost-effective techniques. Accordingly, there is an urgent call for the best use of this neglected source in extensive attempts to convert waste materials into highly useful compounds. To the best of our knowledge, most of the applied nanomaterials have been verified for *in vitro* studies and are limited to lab work only, while investigations of *in vivo* clinical trials have yet to be applied thoroughly. Consequently, further *in vivo* studies are needed and are highly recommended. In addition, the actual action mechanism of the prepared NPs against *M. tuberculosis* is unclear. Moreover, optical nanosensors, which were investigated for tuberculosis detection, should be further developed and constructed on a large scale to be integrated into commercial devices.

6. Conclusion

The current review shed light on the novel nanomaterials required for a rapid and clear diagnosis of the widespread tuberculosis disease. In addition, nanomaterial-based optical sensors could be used as an effective strategy in detection procedures based on SPR, SERS, and fluorescence emission phenomena. Some nanomaterials (*e.g.* Au NPs, Ag NPs, NiO NPs, and CdTe QDs) were reported as efficient optical probes

for constructing successful sensors to be applied in tuberculosis diagnosis. Limitations and future perspectives were also compiled and discussed in the current review paper.

Author contributions

R. M. El-Shabasy: conceptualisation, investigation, visualisation, writing original draft, and writing review and editing. M. Zahran: investigation, writing original draft and writing review and editing. A. H. Ibrahim: review and editing. Y. R. Maghraby: revising and editing. Prof. M. Nayel: conceptualisation, supervision, review and editing.

Conflicts of interest

There are no conflicts to declare.

References

1 N. Usharani, S. V. Kanth and N. Saravanan, *Int. J. Biol. Macromol.*, 2022, **227**, 262–272.
2 W.H.O. Tuberculosis. WHO, Geneva, Switzerland, 2023.
3 W. Lin, S. Fan and K. Liao, *Front. Cell. Infect. Microbiol.*, 2023, 1–15.
4 E. Tenland, A. Pochert, N. Krishnan, K. U. Rao, S. Kalsum, K. Braun, I. Glegola-Madejska, M. Lerm, B. D. Robertson, M. Lindén and G. Godaly, *PLoS One*, 2019, **14**, 1–16.
5 C. Sun, X. Zhang, J. Wang, Y. Chen and C. Meng, *BMC Complementary Med. Ther.*, 2021, 1–7.
6 M. Zahran, R. M. El-Shabasy, A. Elrashedy, W. Mousa, M. Nayel, A. Salama, A. Zaghawa and A. Elsify, *RSC Adv.*, 2023, **13**, 31795–31810.
7 H. S. Schaaf, A. Bekker and H. Rabie, *Front. Public Heal.*, 2023, **11**, 1239734, DOI: **10.3389/fpubh.2023.1239734**.
8 S. Ramón-García, C. Ng, H. Anderson, J. D. Chao, X. Zheng, T. Pfeifer, Y. Av-Gay, M. Roberge and C. J. Thompson, *Antimicrob. Agents Chemother.*, 2011, **55**, 3861–3869.
9 S. Tiberi, M. Muñoz-Torrico, R. Duarte, M. Dalcolmo, L. D'Ambrosio and G.-B. Migliori, *Pulmonology*, 2018, **24**, 86–98.
10 S. Iftikhar and M. Rehan Sarwar, *J. Basic Clin. Pharm.*, 2017, **8**, S131–S136.
11 P. Kulkarni, D. Rawtani and T. Barot, *Colloids Surf., A*, 2019, **565**, 131–142.
12 T. Ganz, *Nat. Rev. Immunol.*, 2003, **3**, 710–720.
13 M. Nasiruddin, M. K. Neyaz and S. Das, *Tuberc. Res. Treat.*, 2017, **2017**, 1–12.
14 P. Dadgostar, *Infect. Drug Resist.*, 2019, **12**, 3903–3910.
15 M. Gajdács and F. Albericio, *Antibiotics*, 2019, **8**, 8–11.
16 I. S. Padda and K. M. Reddy, Antitubercular Medications. [Updated 2023 Jun 3], *In StatPearls [Internet]. Treasure Island (FL), StatPearls Publishing*; 2023. *Available from*: **https://www.ncbi.nlm.nih.gov/books/NBK557666/**.
17 **https://www.merckmanuals.com/professional/infectious-diseases/mycobacteria/tuberculosis-tb**.
18 S. E. Dorman, P. Nahid and E. V. Kurbatova, *N. Engl. J. Med.*, 2021, **384**, 1705–1718.
19 F. Quenard, P. E. Fournier, M. Drancourt and P. Brouqui, *Int. J. Antimicrob. Agents*, 2017, **50**, 252–254.
20 F. Behzad, E. Sefidgar, A. Samadi, W. Lin, I. Pouladi and J. Pi, *Curr. Med. Chem.*, 2022, **29**, 86–98.
21 WHO, 2023. **https://www.who.int/news-room/fact-sheets/detail/tuberculosis**.
22 Y. Saito, N. Yoshii and Y. Kaneko, *BMC Infect. Dis.*, 2019, **19**, 374.
23 J. C. Palomino and A. Martin, *Antibiotics*, 2014, **3**, 317–340.
24 D. Chinemerem Nwobodo, M. C. Ugwu, C. Oliseloke Anie, M. T. S. Al-Ouqaili, J. Chinedu Ikem, U. Victor Chigozie and M. Saki, *J. Clin. Lab. Anal.*, 2022, **36**, 1–10.
25 A. Surendiran, S. Sandhiya, S. C. Pradhan and C. Adithan, *Indian J. Med. Res*, 2009, **130**, 689–701.
26 R. Foulkes, E. Man, J. Thind, S. Yeung, A. Joy and C. Hoskins, *Biomater. Sci.*, 2020, **8**, 4653–4664.
27 D. Rawtani, M. Tharmavaram, G. Pandey and C. M. Hussain, *TrAC, Trends Anal. Chem.*, 2019, **120**, 115661.
28 P. S. Chauhan, M. Kumarasamy, A. Sosnik and D. Danino, *ACS Appl. Mater. Interfaces*, 2019, **11**, 39436–39448.
29 A. V. Zvyagin, X. Zhao, A. Gierden, W. Sanchez, J. A. Ross and M. S. Roberts, *J. Biomed. Opt.*, 2008, **13**, 064031.
30 P. V. Baptista, M. Koziol-Montewka, J. Paluch-Oles, G. Doria and R. Franco, *Clin. Chem.*, 2006, **52**, 1433–1434.
31 Q. Zhang, J. Sun, Y. Wang, W. He, L. Wang, Y. Zheng, J. Wu, Y. Zhang and X. Jiang, *Front. Microbiol.*, 2017, **8**, 1–15.
32 A. Raza, F. B. Sime, P. J. Cabot, F. Maqbool, J. A. Roberts and J. R. Falconer, *Drug Discov. Today*, 2019, **24**, 858–866.
33 V. Perumal, M. S. M. Saheed, N. M. Mohamed, M. S. M. Saheed, S. S. Murthe, S. C. B. Gopinath and J. M. Chiu, *Biosens. Bioelectron.*, 2018, **116**, 116–122.
34 Y. Wang, F. Zhang, J. Liu, B. Yang, Y. Yuan, Y. Zhou and S. Bi, *Spectrochim. Acta, Part A*, 2023, **297**, 122709.
35 H. M. Abdallah, M. H. A. Elella and M. M. Abdel-aziz, *Int. J. Biol. Macromol.*, 2023, **232**, 123394.
36 S. Mitra, S. Kandambeth, B. P. Biswal, M. Abdul Khayum, C. K. Choudhury, M. Mehta, G. Kaur, S. Banerjee, A. Prabhune, S. Verma, S. Roy, U. K. Kharul and R. Banerjee, *J. Am. Chem. Soc.*, 2016, **138**, 2823–2828.
37 S. Alfei and A. M. Schito, *Polymers*, 2020, **12**, 1195.
38 B. N. Patil and T. C. Taranath, *Int. J. Mycobact.*, 2016, **5**, 197–204.
39 C. Mahendra, M. N. Chandra, M. Murali, M. R. Abhilash, S. B. Singh, S. Satish and M. S. Sudarshana, *Process Biochem.*, 2020, **89**, 220–226.
40 K. R. Raghupathi, R. T. Koodali and A. C. Manna, *Langmuir*, 2011, **27**, 4020–4028.
41 B. Baruwati, D. K. Kumar and S. V. Manorama, *Sens. Actuators, B*, 2006, **119**, 676–682.
42 Q. L. Feng, J. Wu, G. Q. Chen, F. Z. Cui, T. N. Kim and J. O. Kim, *J. Biomed. Mater. Res.*, 2000, **52**, 662–668.
43 S. Mohanty, P. Jena and R. Mehta, *et al.*, *Antimicrob. Agents Chemother*, 2013, **57**, 3688–3698.

44 M. Yamanaka, K. Hara and J. Kudo, *Appl. Environ. Microbiol.*, 2005, **71**, 7589–7593.
45 R. Pati, R. K. Mehta, S. Mohanty, A. Padhi, M. Sengupta, B. Vaseeharan, C. Goswami and A. Sonawane, *Nanomedicine*, 2014, **10**, 1195–1208.
46 S. Parveen, T. Sur, S. Sarkar and R. Roy, *Appl. Biochem. Biotechnol.*, 2023, **195**, 3606–3614, DOI: 10.1007/s12010-023-04315-1.
47 J. A. Kumar, T. Krithiga, S. Manigandan, S. Sathish, A. A. Renita, P. Prakash, B. S. N. Prasad, T. R. P. Kumar, M. Rajasimman, A. Hosseini-Bandegharaei, D. Prabu and S. Crispin, *J. Cleaner Prod.*, 2021, **324**, 129198.
48 H. Wang, J. Wei, H. Jiang, Y. Zhang, C. Jiang and X. Ma, *Molecules*, 2021, **26**, 1453, DOI: 10.3390/molecules26051453.
49 A. Khurana, S. Tekula, M. A. Saifi, P. Venkatesh and C. Godugu, *Biomed. Pharmacother.*, 2019, **111**, 802–812.
50 S. Saadat, D. Rawtani and G. Parikh, *J. Drug Delivery Sci. Technol.*, 2022, **76**, 103755.
51 S. Abdelghany, T. Parumasivam, A. Pang, B. Roediger, P. Tang, K. Jahn, W. J. Britton and H. K. Chan, *J. Drug Delivery Sci. Technol.*, 2019, **52**, 642–651.
52 M. H. Abu Elella, E. S. Goda, H. M. Abdallah, M. M. Abdel-Aziz and H. Gamal, *Carbohydr. Polym.*, 2023, **303**, 120443.
53 M. M. Abdel-Aziz, M. H. A. Elella and R. R. Mohamed, *Int. J. Biol. Macromol.*, 2020, **142**, 244–253.
54 M. Zahran, Z. Khalifa, M. A.-H. Zahran and M. Abdel Azzem, *Microchem. J.*, 2021, **165**, 106173.
55 M. Zahran, Z. Khalifa, M. A. H. Zahran and M. Abdel Azzem, *ACS Appl. Nano Mater.*, 2020, **3**, 3868–3875.
56 M. Zahran, Z. Khalifa, M. A. H. Zahran and M. A. Azzem, *Electrochim. Acta*, 2021, **394**, 139152.
57 M. Zahran, Z. Khalifa, M. A. H. Zahran and M. A. Azzem, *Electrochim. Acta*, 2020, **356**, 13685.
58 Z. Khalifa, M. Zahran, M. A.-H. Zahran and M. A. Azzem, *RSC Adv.*, 2020, **10**, 37675–37682.
59 H. K. Abbas and Z. F. Mahdi, *Results Opt.*, 2023, **12**, 100497.
60 W. Kang, H. Lin, R. Jiang, Y. Yan, W. Ahmad, Q. Ouyang and Q. Chen, *Ultrason. Sonochem.*, 2022, **88**, 106095.
61 T. Rasheed, *TrAC, Trends Anal. Chem.*, 2023, **160**, 116957.
62 R. M. Kamel, A. Shahat, M. M. Abd El-Emam and E. M. Kilany, *Spectrochim. Acta, Part A*, 2023, **288**, 122203.
63 A. Samavati, Z. Samavati, A. F. Ismail, N. Yahya, M. H. D. Othman and M. A. Rahman, *Meas. J. Int. Meas. Confed.*, 2021, **167**, 108171.
64 J. Yang, S. Lu, B. Chen, F. Hu, C. Li and C. Guo, *TrAC, Trends Anal. Chem.*, 2023, **159**, 116945.
65 J. Zhang, M. Zhou, X. Li, Y. Fan, J. Li, K. Lu, H. Wen and J. Ren, *Talanta*, 2023, **254**, 124133.
66 S. J. Kahng, S. D. Soelberg, F. Fondjo, J. H. Kim, C. E. Furlong and J. H. Chung, *Biomed. Microdevices*, 2020, **22**, 50.
67 J. Zhang and F. He, *Talanta*, 2022, **236**, 122902.
68 J. Zhang, Y. Li, S. Duan and F. He, *Anal. Chim. Acta*, 2020, **1123**, 9–17.
69 H. J. Kadhim, H. Al-Mumen, H. H. Nahi and S. M. Hamidi, *Optik*, 2022, **269**, 169907.
70 D. Liu and Z. Li, *Opt. Commun.*, 2022, **502**, 127419.
71 P. Srivastava, R. Prakash Ojha, G. Ji and R. Prakash, *Mater. Today Proc.*, 2022, **62**, 3033–3037.
72 S. Thakkar, J. Liu, L. F. Dumée, B. R. Singh, S. Shukla and W. Yang, *J. Water Process Eng.*, 2022, **48**, 102833.
73 C. Maphanga, S. Manoto, S. Ombinda-Lemboumba, Y. Ismail and P. Mthunzi-Kufa, *Sens. Bio-Sensing Res.*, 2023, **39**, 100545.
74 R. Srivastava, S. Pal and Y. K. Prajapati, *Plasmonics*, 2023, **18**, 1–10.
75 A. Radha Pathania, S. Doda, S. Sharma and A. Kundu, *Mater. Today Proc.*, 2023.
76 M. Zahran and A. H. Marei, *Int. J. Biol. Macromol.*, 2019, **136**, 586–596.
77 M. Zahran, Z. Khalifa, M. A. H. Zahran and M. Abdel Azzem, *Mater. Adv.*, 2021, **2**, 7350–7365.
78 I. Dhanya, S. Chandran, L. Mariya Varghese, S. Nithish and S. Reji, *Mater. Today Proc.*, 2020, **43**, 3780–3783.
79 M. T. Alula, S. Krishnan, N. R. Hendricks, L. Karamchand and J. M. Blackburn, *Microchim. Acta*, 2017, **184**, 219–227.
80 S. Tabbasum, M. I. Majeed, H. Nawaz, N. Rashid, M. Tahira, A. Mohsin, A. Arif, A. ul Haq, M. Saleem, G. Dastgir, F. Batool and S. Bashir, *Photodiagn. Photodyn. Ther.*, 2021, **35**, 102426.
81 M. G. Daher, S. A. Taya, A. H. M. Almawgani, A. T. Hindi, I. Colak and S. K. Patel, *Plasmonics*, 2023, **18**, 1–10.
82 S. Subramanian, S. Ganapathy and S. Subramanian, *J. Environ. Chem. Eng.*, 2022, **10**, 106941.
83 D. Du, L. Wang, D. Ding, Y. Guo, J. Xu, F. Qiao, H. Wang and W. Shen, *Chem. Eng. J.*, 2023, **461**, 142040.
84 A. Guo, F. Pei, W. Hu, M. Xia, X. Mu, Z. Tong, F. Wang and B. Liu, *Bioelectrochemistry*, 2023, **150**, 108358.
85 P. Chen, M. Li, W. Peng, T. Liu, J. Huang and B. Ying, *Sens. Actuators, B*, 2023, **376**, 132997.
86 L. Liang, M. Chen, Y. Tong, W. Tan and Z. Chen, *Anal. Chim. Acta*, 2021, **1186**, 339090.
87 W. Ahmad, S. Chandra Bhatt, M. Verma, V. Kumar and H. Kim, *Environ. Nanotechnol., Monit. Manage.*, 2022, **18**, 100674.
88 H. Chen, F. Liu, K. Koh, J. Lee, Z. Ye, T. Yin and L. Sun, *Microchim. Acta*, 2013, **180**, 431–436.
89 H. El-Samadony, A. Althani, M. A. Tageldin and H. M. E. Azzazy, *Expert Rev. Mol. Diagn.*, 2017, **17**, 427–443.
90 R. E. Karunaratne, L. A. Wijenayaka, S. S. Wijesundera, K. M. N. De Silva, C. P. Adikaram and J. Perera, *BMC Infec Dis*, 2019, 1–9.
91 S. Montalvo-Quirós, S. Gómez-Graña, M Vallet-Regí, R. C. Prados-Rosales, B. González and J. L. Luque-Garcia, *Colloids Surf. B: Biointerfaces*, 2021, **197**, 111405.
92 E. Tenland, N. Krishnan, A. Rönnholm, S. Kalsum, M. Puthia, M. Mörgelin, M. Davoudi, M. Otrocka, N. Alaridah, I. Glegola-Madejska, E. Sturegård, A. Schmidtchen, M. Lerm, B. D. Robertson and G. Godaly, *Tuberculosis*, 2018, **113**, 231–238.
93 M. Rajan and V. Raj, *Carbohyd. Polym.*, 2013, **98**, 951–958.
94 R. Amarnath Praphakar, M. Jeyaraj, M. Ahmed, S. Suresh Kumar and M. Rajan, *Int. J. Biol. Macromol.*, 2018, **118**, 1627–1638.